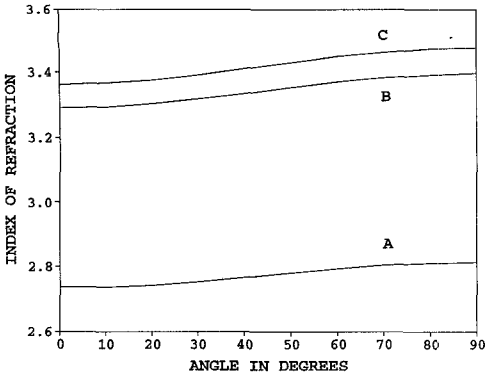

Fig. 5. Effective index of refraction versus angle of the microstrip with $\epsilon_1 = 9.6$, $\epsilon_2 = 10.4$, $\epsilon_3 = 8.2$, $b = 12.7$ mm, $h_1 = 0.5$ mm, $h_2 = 12.2$ mm, $w = 0.5$ mm, and $f = 30$ GHz. (A) $\mu_{xx} = \mu_{yy} = \mu_{zz} = 1.0$, (B) $\mu_{xx} = \mu_{zz} = 1.0$ and $\mu_{yy} = 1.6$, and (C) $\mu_{xx} = 1.0$, $\mu_{yy} = 1.6$, and $\mu_{zz} = 1.8$.

and $[\mu]$ are shown in Fig. 5. The physical dimensions of the guiding structure are the same as those used in earlier microstrip line studies, with the permittivity tensor parameters chosen to be $\epsilon_1 = 9.6$, $\epsilon_2 = 10.4$, and $\epsilon_3 = 8.2$. Dispersion curves A, B, and C show that by changing the material from being magnetically isotropic to magnetically biaxial can increase the effective index of refraction considerably, particularly by varying the μ_{yy} element.

IV. Conclusion

An analysis based on the spectral-domain method was applied to study the effects of misalignment between the principal axes of the substrate and those of the waveguide on the dispersive properties of grounded slotlines, microstrips, and edge coupled lines printed on anisotropic substrates. The newly derived expression for the Green's function is written explicitly in terms of both $[\epsilon]$ and $[\mu]$ tensor elements, with the off-diagonal elements of the permittivity also included in the formulation. The dispersion characteristics of these transmission lines are examined when they are printed on dielectrically biaxial substrates. Numerous results are provided for different medium parameters for frequencies up to 40.0 GHz when angles of axes rotation of the permittivity tensor change from 0° to 90°. Also, the variation in the index of refraction is examined for a microstrip line printed on a substrate which is characterized simultaneously by both its permittivity and permeability tensors. It is observed that misalignment effects on the dispersion properties of MIC's cannot be ignored, even at the lower frequencies for some anisotropic substrate materials.

References

[1] R. P. Owens, J. E. Itken, and T. C. Edwards, "Quasi-static characteristics of microstrip on an anisotropic sapphire substrate," *IEEE Trans. Microwave Theory Tech.*, vol. MTT-24, pp. 499–505, Aug. 1976.

[2] A-M. A. Al-Sherbiny, "Hybrid mode analysis of microstrip lines on anisotropic substrates," *IEEE Trans. Microwave Theory Tech.*, vol. MTT-29, pp. 1261–1265, Dec. 1981.

[3] N. G. Alexopoulos and C. M. Krowne, "Characteristics of single and coupled microstrips on anisotropic substrates," *IEEE Trans. Microwave Theory Tech.*, vol. MTT-26, pp. 387–393, June 1978.

[4] A. Nakatani and N. G. Alexopoulos, "Toward a generalized algorithm for the modeling of the dispersive properties of integrated circuit structures on anisotropic substrates," *IEEE Trans. Microwave Theory Tech.*, vol. MTT-33, pp. 1436–1441, Dec. 1985.

[5] H. Y. Yang and N. G. Alexopoulos, "Uniaxial and biaxial substrate effects of finline characteristics," *IEEE Trans. Microwave Theory Tech.*, vol. MTT-33, pp. 24–29, Jan. 1987.

[6] J. L. Tsalamengas, N. K. Uzunoglu, and N. G. Alexopoulos, "Propagation characteristics of a microstrip line printed on a general anisotropic substrate," *IEEE Trans. Microwave Theory Tech.*, vol. MTT-33, pp. 941–945, Oct. 1985.

[7] A. A. Mostafa, C. M. Krowne, and K. A. Zaki, "Numerical Spectral Matrix method for propagation in general layered media: application to isotropic and anisotropic substrates," *IEEE Trans. Microwave Theory Tech.*, vol. MTT-35, pp. 1399–1407, Dec. 1987.

[8] T. Q. Ho and B. Beker, "Spectral domain analysis of shielded microstrip lines on biaxially anisotropic substrates," *IEEE Trans. Microwave Theory Tech.*, vol. 39, pp. 1017–1021, June 1991.

[9] T. Itoh and R. Mittra, "A technique for computing dispersion characteristics of shielded microstrip lines," *IEEE Trans. Microwave Theory Tech.*, vol. MTT-22, pp. 896–898, Oct. 1974.

[10] L. Schmidt and T. Itoh, "Spectral domain analysis of dominant and higher order modes in finlines," *IEEE Trans. on Microwave Theory Tech.*, vol. MTT-28, pp. 981–985, Sept. 1980.

[11] T. Q. Ho, "Guided wave propagation in millimeter-wave integrated circuits using anisotropic materials," Ph.D. dissertation, University of South Carolina, Columbia, SC, Dec. 1991.

Analysis of an Infinite Array of Rectangular Anisotropic Dielectric Waveguides Using the Finite-Difference Method

Carlos Leônidas da Silva Souza Sobrinho and Attílio José Giarola

***Abstract*—The finite-difference method is used in the analysis of the propagation characteristics of an infinite array of rectangular dielectric waveguides. Particular attention is devoted to the mode coupling analysis and a comparison with results from an integral equation method is presented. The wave equation is solved in terms of the transverse components of the magnetic field, resulting in an eigenvalue problem with the elimination of spurious modes. The formulation is general and may be applied to the solution of other problems, including those with anisotropic dielectrics and with a continuous variation of the index of refraction profile in the wavegide cross section.**

I. Introduction

The practical application of dielectric waveguide in millimeter-wave and optical integrated circuits depends critically on the propagation characteristics of these waveguides. For this reason, there has been increased interest in methods of determining these characteristics for practical dielectric waveguiding structures. The point-matching method was used to analyze the two-layer rectangular cross section waveguide [1]. The use of the finite-element method became attractive after the elimination of the spurious modes [2] and because of its potential of solving nonhomogeneous and anisotropic waveguides [3], [4]. The elimination of the spurious modes of the finite-difference method has also enhanced the

Manuscript received May 29, 1991; revised October 25, 1991. This work was partially supported by the following Brazilian agencies: CAPES, CNPq, TELEBRÁS, and FINEP.

C. L. da Silva Souza Sobrinho is with the Electrical Engineering Department, Federal University of Para (UFPa), P.O. Box 918, CEP 66050, Belem, PA, Brazil.

A. J. Giarola is with School of Electrical Engineering, State University of Campinas (UNICAMP), P.O. Box 6101, CEP 13081, Campinas, SP, Brazil.

IEEE Log Number 9106773.

interest of using this method for solving dielectric waveguides. Bierwirth *et al.* [5] and Schulz *et al.* [6], by solving the wave equation in terms of the transverse components of the magnetic field, were able to obtain solutions with the exclusion of spurious modes. While the analysis developed by Bierwirth *et al.* [5] was applicable to dielectric waveguides having refractive step index profiles in their cross sections, Schulz *et al.* [6] have extended the analysis to include waveguide with graded-index profiles. In their analysis, however, they have assumed isotropic dielectrics.

One of the objectives of this paper is to extend these previous analyses to include dielectric anisotropy. The formulation is developed for cylindrical dielectric waveguide structures with an arbitrarily varying index of refraction profile over their entire cross sections. The analysis is general and is applicable to biaxial anisotropic dielectrics. The magnetic permeability is assumed to be constant and equal to the free-space value ($\mu = \mu_o$).

In this analysis, the vector wave equation is solved in terms of the transverse magnetic field components, H_x and H_y, such that the spurious modes are eliminated by an implicit inclusion of the condition that the divergence of the magnetic field has to be equal to zero ($\nabla \cdot \overline{H} = 0$) [5], [6].

This wave equation is solved numerically by using the finite-difference method for each of the four regions of the five-point mesh shown in Fig. 1, by taking into account the boundary conditions existing in the interface of regions 1, 2, 3, and 4, as well as in the boundaries that limit the waveguide region. The problem is reduced to a conventional eigenvalue problem.

The use of a graded mesh, as shown in Fig. 2, allows an improvement in the precision of the calculated results without increasing the number of mesh points. This is done by using a more refined discretization in the most critical regions with a compromise in the regions where there is a more regular behavior.

The boundaries that limit the waveguide region, as shown in Fig. 2, should be positioned far enough away in order not to perturbe the results desired for the unbounded case. However, by setting near electric or magnetic boundaries we may be able to investigate the coupled modes of an infinite array of dielectric waveguides. Numerical results were compared with those obtained by Yang *et al.* [7] using an integral equation analysis.

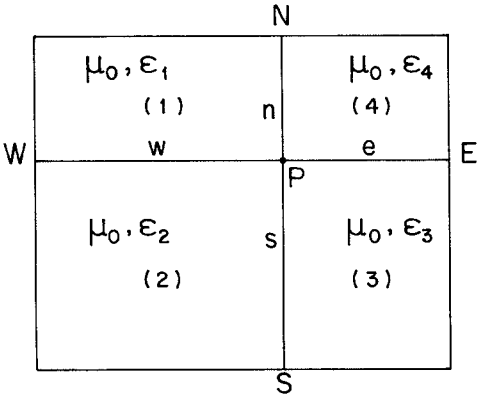

Fig. 1. Graded mesh of the five-point representation.

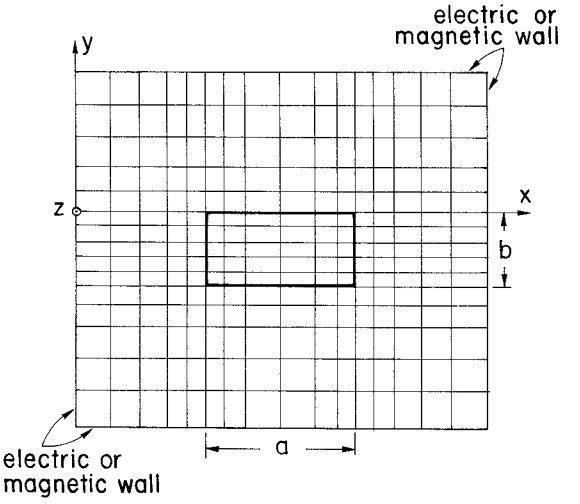

Fig. 2. Graded mesh of the finite-difference representation.

II. Theory

General anisotropic dielectrics will be considered in the analysis. However, they will be oriented in such a way that the optical axes coincide with the x, y and z coordinate directions shown in Fig. 2. Thus, for nonuniform biaxial anisotropic dielectric, the permittivity tensor is diagonal, with components $\epsilon_x(x, y)$, $\epsilon_y(x, y)$ and $\epsilon_z(x, y)$ with a magnetic permeability equal to that of free space, $\mu = \mu_o$. The fields are assumed to have a harmonic time dependence of the type exp ($j\omega t$) and to propagate along the z direction with a z dependence given by exp ($-\gamma_z z$), where ω the angular frequency and γ_z is the propagation constant.

The vector wave equation, describing the wave propagation along a cylindrical waveguide with a nonhomogeneous cross section and anisotropic dielectric material, may be obtained from Maxwell's equations, resulting:

$$-[\epsilon]^{-1}\nabla^2\overline{H} + [\nabla([\epsilon]^{-1})] \times (\nabla \times \overline{H}) = \omega^2\mu\overline{H}. \quad (1)$$

In order to simplify the solution of the problem, the vector wave equation (1) may be written in terms of the transverse components of the magnetic field, H_x and H_y, such that the problem may be transformed into a conventional eigenvalue problem. As a result, the following coupled wave equations are obtained:

$$\frac{\epsilon_\alpha(x, y)}{\epsilon_z(x, y)}\frac{\partial^2}{\partial\alpha^2}H_\tau + \frac{\partial^2}{\partial\tau^2}H_\tau + \frac{\epsilon_z(x, y) - \epsilon_\alpha(x, y)}{\epsilon_z(x, y)}\frac{\partial^2}{\partial\tau\,\partial\alpha}H_\alpha + \frac{\epsilon_\alpha(x, y)}{\epsilon_z^2(x, y)}\frac{\partial}{\partial\alpha}\epsilon_z(x, y)\left[\frac{\partial}{\partial\tau}H_\alpha - \frac{\partial}{\partial\alpha}H_\tau\right] + \left[k_o^2\frac{\epsilon_\alpha(x, y)}{\epsilon_o} + \gamma_z^2\right]H_\tau = 0, \quad (2)$$

where $\alpha = x$ when $\tau = y$ and $\alpha = y$ when $\tau = x$, ϵ_o is the free-space permittivity and $k_o = \omega\sqrt{\mu_o\epsilon_o}$ is the free-space wavenumber.

In order to eliminate the spurious modes, the divergence of the magnetic field equal to zero ($\nabla \cdot \overline{H} = 0$) was included in the formulation of (1) and in the calculation of the longitudinal component of the magnetic field [5], [6]:

$$H_z = \frac{1}{\gamma_z}\left[\frac{\partial}{\partial x}H_x + \frac{\partial}{\partial y}H_y\right], \quad (3)$$

which was used to satisfy one of the boundary conditions.

In order to develop the finite-difference method, a graded mesh of points is drawn in the waveguide cross section as shown in Fig. 2. Thus, a generic point P_i is distant from its four neighbor points to the north, south, east or west by n, s, e, or w, respectively, as shown in Fig. 1. The coupled equations (2) are used to write the

field equations around any one of the points P_i, two for each region 1, 2, 3, and 4, as shown in Fig. 1. These eight equations are summarized in the following expression:

$$
\begin{aligned}
0 = &-\frac{m_{q\tau}}{m_{i\alpha}} H_{\alpha M_{i\alpha}} - \frac{m_{i\alpha}}{m_{q\tau}} \frac{\epsilon_{\tau j}}{\epsilon_{zj}} \left[1 \pm m_{q\tau} \frac{\epsilon_{z\tau j}}{2\epsilon_{zj}}\right] H_{\alpha M_{q\tau}} \\
&+ \left[\frac{m_{i\alpha}}{m_{q\tau}} \frac{\epsilon_{\tau j}}{\epsilon_{zj}} \left(1 \pm m_{q\tau} \frac{\epsilon_{z\tau j}}{2\epsilon_{zj}}\right) + \frac{m_{q\tau}}{m_{i\alpha}}\right] H_{\alpha p} \\
&- \frac{1}{2} m_{q\tau} m_{i\alpha} [\omega^2 \mu \epsilon_{\tau j} + \gamma_z^2] H_{\alpha p} \\
&+ \left[\pm m_{q\tau} \frac{\epsilon_{\tau j}}{2\epsilon_{zj}^2} \epsilon_{z\tau j} \pm \frac{\epsilon_{zj} - \epsilon_{\tau j}}{4\epsilon_{zj}}\right] H_{\tau M_{i\alpha}} \\
&\pm \frac{\epsilon_{zj} - \epsilon_{\tau j}}{4\epsilon_{zj}} H_{\tau M_{q\tau}} + \left[\pm m_{q\tau} \frac{\epsilon_{\tau j} \epsilon_{z\tau j}}{2\epsilon_{zj}^2} \pm \frac{\epsilon_{zj} - \epsilon_{\tau j}}{2\epsilon_{zj}}\right] H_{\tau p} \\
&\pm m_{i\alpha} \frac{\epsilon_{\tau j}}{\epsilon_{zj}} H_{\alpha \tau j} \pm m_{q\tau} H_{\alpha \alpha j},
\end{aligned} \tag{4}
$$

where

$$
\begin{aligned}
&m_{i\alpha} = w, e; \quad m_{q\tau} = n, s; \quad M_{i\alpha} = W, E; \quad M_{q\tau} = N, S; \\
&\quad \text{for } \alpha \text{ when } \tau = y \text{ and } m_{i\alpha} = n, s; \quad m_{q\tau} = w, e; \\
&\quad M_{i\tau} = N, S; \quad M_{q\tau} = W, E; \text{ for } \alpha = y \text{ when } \tau = x. \\
&\epsilon_{z\tau j} = \left.\frac{\partial \epsilon_z}{\partial \tau}\right|_j; \quad H_{\alpha \tau j} = \left.\frac{\partial H_\alpha}{\partial \tau}\right|_j; \quad H_{\alpha \alpha j} = \left.\frac{\partial H_\alpha}{\partial \alpha}\right|_j \quad \text{with } j = 1, 2, 3, 4
\end{aligned}
$$

representing regions 1, 2, 3, and 4, shown in Fig. 1, respectively; i and q correspond to the following values: $(i, q) = (1, 1), (1, 2), (2, 2), (2, 1)$ with $\alpha = x$ when $\tau = y$ and $(i, q) = (1, 1), (2, 1), (2, 2), (1, 2)$ with $\alpha = y$ when $\tau = x$, for regions 1, 2, 3, and 4 (Fig. 1), respectively.

At the interface between the four regions of the graded mesh of five points, as shown in Fig. 1, the boundary conditions that require the continuity of the longitudinal components of the electric field, E_z, and of the magnetic field, H_z, are then imposed. From these conditions we obtain relations between the derivatives of the transverse components of the magnetic field, H_x and H_y. From the various sets of possible relations [5] we have chosen for H_x, the following: $E_{z1} = E_{z2}$, $E_{z3} = E_{z4}$, $H_{z1} = H_{z2}$, $H_{z3} = H_{z4}$, $H_{z1} = H_{z4}$ and for H_y we have chosen: $E_{z1} = E_{z4}$, $E_{z2} = E_{z3}$, $H_{z1} = H_{z4}$, $H_{z2} = H_{z3}$, $H_{z1} = H_{z2}$. As a result, similar expressions as those given by Bierwirth *et al.* [5] are obtained.

The set of coupled equations (4), along with this set of relations lead to the desired solution of the wave equation. After some manipulation of this set of equations, the following coupled equations are obtained:

$$
\begin{aligned}
&\sum_{i=W,E,N,S} A_i H_{xi} + \sum_{i=W,E,N,S} B_i H_{yi} + A_p H_{xp} + B_p H_{yp} \\
&\quad + \gamma_z^2 A_{p\gamma} H_{xp} + \gamma_z^2 B_{p\gamma} H_{yp} = 0,
\end{aligned} \tag{5}
$$

$$
\begin{aligned}
&\sum_{i=W,E,N,S} C_i H_{yi} + \sum_{i=W,E,N,S} D_i H_{xi} + D_p H_{xp} + C_p H_{yp} \\
&\quad + \gamma_z^2 D_{p\gamma} H_{xp} + \gamma_z^2 C_{p\gamma} H_{yp} = 0,
\end{aligned} \tag{6}
$$

where the coefficients A_i, B_i, C_i, D_i $(i = W, E, N, S)$, A_p, $A_{p\gamma}$, B_p, $B_{p\gamma}$, C_p, $C_{p\gamma}$, D_p and $D_{p\gamma}$ are expressions given in terms of geometrical parameters and the electromagnetic parameters of the dielectric media.

The equations (5) and (6) may be uncoupled in terms of $\gamma_z^2 H_{xp}$ and $\gamma_z^2 H_{yp}$. The result is

$$
\sum_{i=W,E,N,S} D^i H_{xi} + \sum_{i=W,E,N,S} C^i H_{yi} + D^p H_{xp} + C^p H_{yp} = -\gamma_z^2 H_{yp}, \tag{7}
$$

$$
\sum_{i=W,E,N,S} A^i H_{xi} + \sum_{i=W,E,N,S} B^i H_{yi} + A^p H_{xp} + B^p H_{yp} = -\gamma_z^2 H_{xp}, \tag{8}
$$

where

$$
\begin{aligned}
&A^i = (A_i C_{p\gamma} - D_i B_{p\gamma})/D; \quad B^i = (B_i C_{p\gamma} - C_i B_{p\gamma})/D; \\
&A^p = (A_p C_{p\gamma} - D_p B_{p\gamma})/D; \quad B^p = (B_p C_{p\gamma} - C_p B_{p\gamma})/D; \\
&D^i = (D_i A_{p\gamma} - A_i D_{p\gamma})/D; \quad C^i = (C_i A_{p\gamma} - B_i D_{p\gamma})/D; \\
&D^p = (D_p A_{p\gamma} - A_p D_{p\gamma})/D; \quad C^p = (C_p A_{p\gamma} - B_p D_{p\gamma})/D; \\
&D = A_{p\gamma} C_{p\gamma} - D_{p\gamma} B_{p\gamma}.
\end{aligned} \tag{9}
$$

Note that, for the graded mesh of Fig. 2 containing N points, there should be N unknowns H_{xp} and N unknowns H_{yp}, one for each point P of the mesh. On the other hand, we may write one equation (7) and one equation (8) for each mesh point, such that a total of $2N$ equations will result from the use of (7) and (8) in the entire mesh. We have therefore an equal number of equations and unknowns. Obviously, in order to be able to solve the numerical problem, N has to be a finite number. This may be accomplished by confining the cross section of the waveguide within electric or magnetic walls.

After defining the graded mesh of points of Fig. 2 and chosen the walls that limit the waveguide cross section, (7) and (8) may be invoked at each mesh point, using the proper boundary conditions at the electric and/or magnetic walls. A system of linear homogeneous equations results that may be written as a conventional eigenvalue problem [5], [6]:

$$
[(A) - \lambda(U)](X) = 0, \tag{10}
$$

where $\lambda = -\gamma_z^2$, (U) is the unit matrix, (X) is the eigenvector, and (A) is a square matrix with coefficients $a_{i,j}$, $b_{i,j}$, $c_{i,j}$ and $d_{i,j}$.

The eigenvalues λ and the eigenvectors (X) may be obtained using the Eispack program [5].

III. Results

The formulation presented here is used in the analysis of the propagation characteristics of an infinite array of rectangular dielectric waveguides having a cross section as shown in Fig. 3. Note that each rectangular dielectric waveguide has dimensions a and b, with a relative dielectric permittivity ϵ_c and a magnetic permeability, μ_o. For an anisotropic dielectric, ϵ_c is a tensor quantity. The medium that surrounds the rectangular dielectric waveguides is a dielectric with a relative dielectric permittivity, ϵ_1, and a magnetic permeability, μ_o. Due to the periodicity of the structure it is sufficient that only one cell of the array be examined. This cell is shown in Fig. 3 with sides A and B. Note, in addition, this cell has symmetry with respect to the 2-3 and 3-4 axes. Therefore, only the cell delimited by the points 1-2-3-4 has to be examined, with the appropriate choice of electric or magnetic walls at the edges of this cell. Depending on the choice of the walls along 2-3 and 3-4, four mode groups may be formed. The first group is defined as the one with an electric wall along 2-3 and a magnetic wall along 3-4. The second and third-groups have only electric and only magnetic walls,

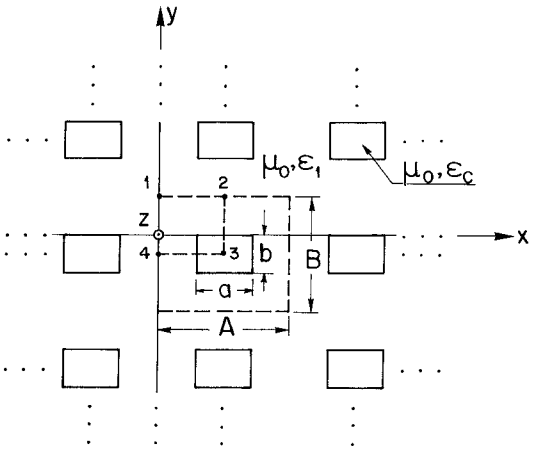

Fig. 3. Cross section of an infinite array of rectangular dielectric waveguides.

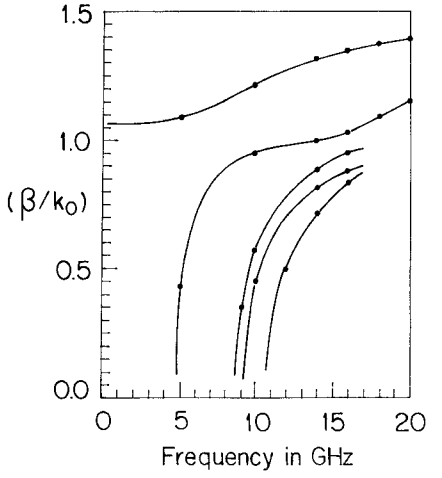

Fig. 4. Normalized phase constant of the first five modes of the first group, as a function of frequency. Also shown are results obtained by Yang *et al.* [7]. $\epsilon_1 = 1.0$, $\epsilon_c = 2.25$, $a = 2.324$ cm, $b = 1.162$ cm, $A = 6.0$ cm and $B = 3.0$ cm.

respectively. The fourth group is obtained by exchanging the electric and magnetic walls of the first group [7].

The normalized phase constants as a function of frequency, expressed in GHz, are shown in Figs. 4 and 5 for the first and fourth groups, respectively. For both cases, isotropic dielectrics were used, with $\epsilon_1 = 1.0$ and $\epsilon_c = 2.25$ and the dimensions were chosen as a = 2.324 cm, $b = 1.162$ cm, $A = 6.0$ cm and $B = 3.0$ cm [7]. The first five modes are shown with solid lines. Results obtained by Yang *et al.* [7] using the integral equation method are also shown with dots. Note the agreement observed with the comparison of both results.

In order to examine the effect of dielectric anisotropy, the rectangular dielectric waveguides with $\epsilon_c = 2.19$ were replaced by uniaxial anisotropic dielectrics with the optical axis along the y-direction. For one case we have chosen $\epsilon_{cx} = \epsilon_{cz} = 2.31$ and $\epsilon_{cy} = 2.19$ and for the other case, $\epsilon_{cx} = \epsilon_{cz} = 2.19$ and $\epsilon_{cy} = 2.31$. The results are shown in Fig. 6. Note that, for $\epsilon_{cy} = 2.31$ (asterisks), the results almost coincide with those for $\epsilon_c = 2.19$ (solid line). For $\epsilon_{cy} = 2.19$ (dotted line) the normalized phase constants are slightly higher than those for $\epsilon_c = 2.19$. Not shown in Fig. 6 are the results that were calculated for the optical axis along the x direction and with $\epsilon_{cy} = \epsilon_{cz} = 2.19$ and $\epsilon_{cx} = 2.31$. These results

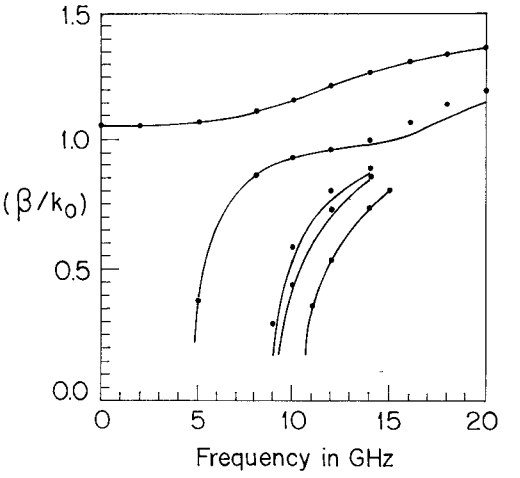

Fig. 5. Same as in Fig. 4, for the fourth group instead of the first group. Also shown are results obtained by Yang *et al.* [7].

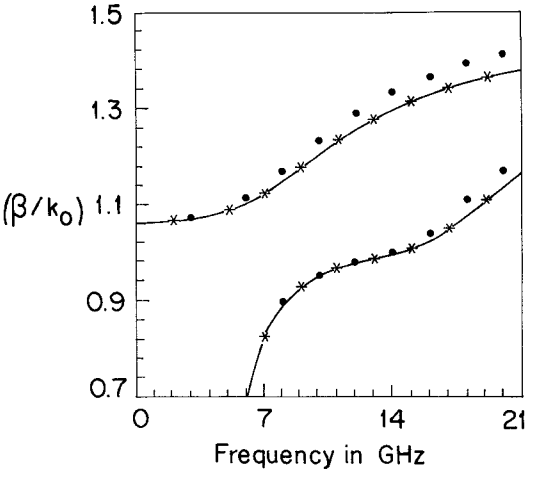

Fig. 6. Normalized phase constant of the first two modes of the first group, as a function of frequency for: (a) isotropic dielectric waveguides with $\epsilon_c = 2.19$ (solid line); (b) anisotropic dielectric waveguides with $\epsilon_{cx,z} = 2.31$ and $\epsilon_{cy} = 2.19$ (dotted line); and (c) anisotropic dielectric waveguides with $\epsilon_{cy,z} = 2.19$ and $\epsilon_{cy} = 2.31$ (asterisks). $\epsilon_1 = 1.0$, $a = 2.324$ cm, $b = 1.162$ cm, $A = 6.0$ cm and $B = 3.0$ cm.

were very similar to those calculated for $\epsilon_{cx} = \epsilon_{cz} = 2.31$ and $\epsilon_{cy} = 2.19$.

IV. Conclusion

The dispersion characteristics of an infinite array of rectangular dielectric waveguides, using isotropic or anisotropic dielectrics were examined using the finite-difference method. In the formulation the vector wave equation, written in terms of the transverse components of the magnetic field, is reduced to a conventional eigenvalue problem. The elimination of spurious modes is accomplished by including the condition that the divergence of the magnetic field is equal to zero. The results obtained for isotropic dielectrics were compared with those obtained using the integral equation method and good agreement was observed for the first five modes.

References

[1] C. Hafner and R. Ballisti, "Electromagnetic waves on cylindrical structures calculated by the method of moments and by the point

matching technique," in *Int. IEEE AP-S Symp. Dig.*, June 1981, pp. 331-333.
[2] M. Koshiba, K. Hayata, and M. Suzuki, "Vectorial finite-element method without spurious solutions for dielectric waveguide problems," *Electron. Lett.*, vol. 20, no. 10, pp. 409-410, May 1984.
[3] K. Hayata, M. Koshiba, M. Eguchi, and M. Suzuki, "Vectorial finite-element method without any spurious solutions for dielectric waveguiding problems using transverse magnetic-field component," *IEEE Trans. Microwave Theory Tech.*, vol. MTT-34, pp. 1120-1124, Nov. 1986.
[4] M. Koshiba, K. Hayata, and M. Suzuki, "Approximate scalar finite-element analysis of anisotropic optical waveguides," *Electron. Lett.*, vol. 18, no. 10, pp. 411-412, May 13, 1982.
[5] K. Bierwirth, N. Schulz, and F. Arndt, "Finite-difference analysis of rectangular dielectric waveguide structures," *IEEE Trans. Microwave Theory Tech.*, vol. MTT-34, pp. 1104-1114, Nov. 1986.
[6] N. Schulz, K. Bierwirth, F. Arndt, and U. Köster, "Finite-difference method without spurious solutions for the hybrid-mode analysis of diffused channel waveguides," *IEEE Trans. Microwave Theory Tech.*, vol. 38, pp. 722-729, June 1990.
[7] H. Yang, J. A. Castaneda, and N. G. Alexopoulos, "An integral equation analysis of an infinite array of rectangular dielectric waveguides," *IEEE Trans. Microwave Theory Tech.*, vol. 38, no. 7, pp. 873-880, July 1990.

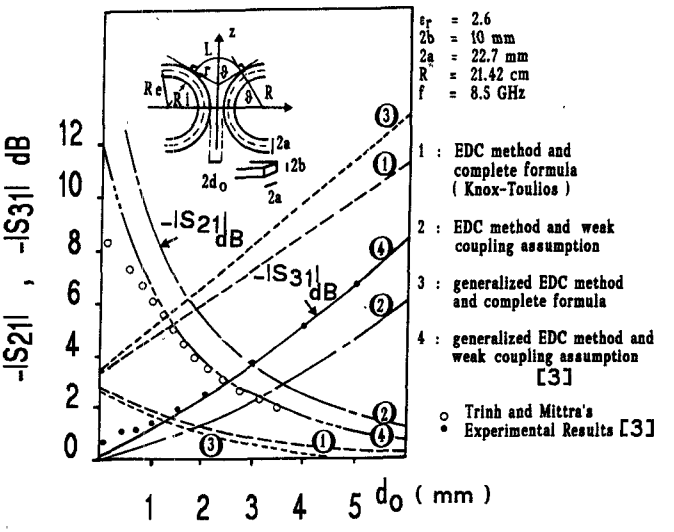

Fig. 1. Scattering coefficients in the case of a symmetric coupler.

Analysis of Coupling in Image Guide Technology

D. L. Paul, M. Habibi, J. Castrillo, Ph. Gelin, and S. Toutain

***Abstract*—Coupling for symmetrical and asymmetrical structures in image guide technology is described. Starting from Trinh and Mittra's analysis, we propose some improvements for treating strong coupling between an image guide and a ring resonator of any radius of curvature, by taking into account the field displacement effect, and for a nonsymmetric coupler, the difference between the propagation constants of the straight and curved image guides. A comparison between this analysis and Trinh and Mittra's experiments has been made.**

I. Introduction

In recent years, greater interest has been paid to millimeter-wave dielectric propagation media for use both in active and passive devices [1]. Derived from guides widely used in optics, these structures are indeed well suited to high frequency bands. When associated with dielectric ring resonators, dielectric waveguides are especially suitable for the modelling of filters [2]. In order to design filters in image guide technology at millimeter wavelengths, it is necessary to characterize accurately the coupling between basic elements.

This paper presents numerous improvements which can be applied to the analysis proposed by Trinh and Mittra for symmetric and nonsymmetric couplers [3] and which are able to predict both the amplitude and the phase of the scattering parameters without any restrictive assumption. To do this, the analysis takes into account not only the shift of the electromagnetic field due to the curvature of the guide but also, in the case of nonsymmetric couplers, the difference in the propagation constants between curved and straight guides. A slight concordance is observed between our theory and Trinh and Mittra's experimental results.

Manuscript received July 31, 1990; revised September 10, 1991.
D. L. Paul, J. Castrillo, Ph. Gelin, and S. Toutain are with Department ENST de Bretagne, BP 832, 29285, Brest Cedex, France.
M. Habibi is with Laboratoire Electronique et Communications, Ecole Mohammadia d'Ingénieurs, BP 765 Rabat, Morocco.
IEEE Log Number 9106776.

II. Trinh and Mittra's Analysis

In the case of a symmetric coupler (Fig. 1), this approach is able to predict scattering coefficients with quite satisfactory accuracy. Their theory is based on three assumptions:

a) The authors assume the radius R to be large enough compared to the wavelength, to neglect the field displacement in the curved structures [4] and approximate the phase constant in this section by the one obtained in a straight section.

b) They use the generalized EDC method (Effective Dielectric Constant) to obtain both the phase constant of the single image guide fundamental mode and the even and odd phase constants of coupled image guides.

c) They suppose that the coupling is weak. From a mathematical point of view, this assumption permits the use of analytical asymptotic equations to derive the even and odd phase constants of the coupler.

To analyze the validity of these hypotheses, we plotted (Fig. 1) the S-parameters versus the spacing between guides for each combination of the techniques available, i.e., for both strong (resolution of Knox and Toulios's transcendental equations [5]) and weak coupling. This figure shows that the results may be very different according to the technique chosen (EDC [5] or generalized EDC method [3]) and that paradoxically Trinh and Mittra's experiments and theoretical results (curve 4, Fig. 1) agree well for strong coupling where the asymptotic equations are not valid.

When applied to a nonsymmetric coupler, the main drawback of Trinh and Mittra's model lies in the necessity of introducing a correction factor into the calculations to model the phase constant difference between straight and curved guides.

Concluding Remark: If the assumption of "weak coupling" in Knox and Toulios's transcendental equations leads to fairly good results concerning symmetric couplers, this may not be significant. Indeed, the excess of coupling obtained when the distance between guides is supposed to be infinite may make up for the omission of the shift of the maximum field amplitude towards the outside of the guide observed in curved structures [4].

Thus, it seems more realistic to take into account this physical phenomenon without assuming a weak coupling approximation and, in the case of nonsymmetric couplers, the difference in propagation